Séminaire Poincaré XIV (2010) 89 – 114 Séminaire Poincaré

Discrete graphs - a paradigm model for quantum chaos

Uzy Smilansky
Department of Physics of Complex Systems
The Weizmann Institute of Science
76100 Rehovot, Israel
and
School of Mathematics
Cardiff University
Cardiff, Wales, United Kingdom

1 Introduction

The question "What is Quantum Chaos ?" seems to be best replied by an operational answer : The research in Quantum Chaos attempts to uncover the finger-prints of classical chaotic dynamics in the corresponding quantum description. In particular, since many attributes of classical (Hamiltonian) chaos are universal, quantum chaos attempts to focus on analogous, but not necessarily the same universal features. One of the most fruitful approaches in the development of classical chaos was to focus on toy models, which are simple enough to allow detailed analysis, without losing the essential dynamical complexity which marks chaotic systems. This same route was followed in Quantum Chaos - some of the toy models were constructed by quantizing the classical toy models. Other models went further and devised leaner and leaner problems which allowed deeper penetration into the essential ingredients of Quantum Chaos. In the present talk I shall describe a recent model - the Laplacian on d-regular graphs - which would seem at first sight as pushing the strife for simplicity *ad absurdum*. However, this is not the case, and by presenting the model, I shall explain by analogy the corresponding concepts which prevail in quantum chaos. It will also give me a chance to comment on the fruitful interaction of quantum chaos research with other fields of Mathematical Physics.

This review is based on the work performed during the past three years by Yehonatan Elon, Amit Godel, Idan Oren and the author. The original papers and thesis [1, 2, 3, 4, 5, 6, 7, 8] contain much more data, results and proofs, and the interested reader is referred there for the information which is lacking here. Our attention to d-regular graphs was brought by the pioneering work of Jakobson *et. al.* [9] which will be discussed at length in the sequel. Previous attempts to relate quantum chaos to combinatorial graphs (not necessarily d-regular) are described in [10].

1.1 The Model : d-regular graphs

Deferring formal definitions to a later stage, the objects of this study are the d-regular graphs on V vertices. These are graphs where each vertex is connected to precisely d other vertices (no loops and no parallel edges). They have very attractive properties which made them very popular in various fields, ranging from computer

science to number theory (see [11] for a review). Their most prominent feature is that they are **expanders** - a concept which can be explained through their geometrical and dynamical properties.

From the geometrical point of view, an expanding graph has the property that the volume of any ball is proportional to that of its boundary. Thus, when V increases, the growing rate of the graph is exponential, hence the name 'expander'.

From the dynamical point of view, a random walker on the graph would visit the vertices with uniform probability exponentially fast. The mixing rate is completely determined by the spectrum of the graph Laplacian to be defined below. It can be easily shown that for connected (non bipartite) d-regular graphs the equilibrium state is reached exponentially fast and at a rate which is independent of V.

The spectral theory of graphs shows that both features can be traced to the same root - namely, the expansion parameter and the mixing rate are related through an inequality attributed to Cheeger [12, 13, 14]. This will not be discussed here any further.

Besides of being expanders, d-regular graphs have another important property of a more local nature :

The local tree structure : Inside a ball of radius $\log_{d-1} V$ about most of its vertices, the local structure of a d-regular graph is identical to that of a d-regular tree. Stated differently, loops of lengths shorter than $\log_{d-1} V$ are rare on the graph.

The spectrum of the d-regular graphs and the corresponding eigenvectors in the limit $V \to \infty$ share many properties with their counterparts in quantum chaos. To introduce them systematically a few concepts and facts should be defined and stated.

1.2 Definitions and facts

A graph G is a set $\mathcal{V}$ of vertices connected by a set $\mathcal{E}$ of edges. The number of vertices is denoted by $V = |\mathcal{V}|$ and the number of edges is $E = |\mathcal{E}|$. A *simple graph* is a graph where an edge cannot connects a vertex to itself, nor can it connect already connected vertices. The connectivity of the graph is specified by the $V \times V$ *adjacency* (*connectivity*) matrix A,

$$A_{i,j} = \begin{cases} 1 & (i,j) \text{ connected} \\ 0 & (i,j) \text{ not connected} \end{cases} \tag{1}$$

We shall deal with *d-regular graphs* where each vertex is connected to exactly d vertices, d stands for the *degree*.

The ensemble of all simple, d-regular graphs with V vertices will be denoted by $\mathcal{G}_{V,d}$. The cardinality of $\mathcal{G}_{V,d}$ increases faster than exponentially in V. Therefore the density of disconnected graphs in $\mathcal{G}_{V,d}$ vanishes in the limit of large V. Averaging over $\mathcal{G}_{V,d}$ will be carried out with uniform probability and will be denoted by $\langle \cdots \rangle$.

While the vertices can be considered as a discrete version of classical *configuration space* for the dynamics on the graph, the *directed edges*, $e = (i,j)$ provide a description of the graph which is the discrete analogue of *phase-space*. It is convenient to associate with each directed edge $e = (j,i)$ its *origin* $o(e) = i$ and *terminus* $t(e) = j$ so that e points from the vertex i to the vertex j. The edge e' follows e if $t(e) = o(e')$. The reverse edge of e will be denoted by $\hat{e} = (i,j)$. The phase-space

connectivity of the graph can be specified by the $2E \times 2E$ matrix B :

$$B_{e',e} = \begin{cases} 1 & o(e') = t(e) \\ 0 & o(e') \neq t(e) \end{cases} \tag{2}$$

Classical trajectories are replaced here by walks on the graph. A *walk* of length t from the vertex x to the vertex y on the graph is a sequence of successively connected vertices $x = v_1, v_2, \cdots, v_t = y$. Alternatively, it is a sequence of $t-1$ directed edges $e_1, \cdots, e_{t-1}$ with $o(e_i) = v_i,\ t(e_i) = v_{i+1}, o(e_1) = x,\ t(e_{v-1}) = y$. A *closed walk* is a walk with $x = y$. The number of walks of length t between x and y equals $(A^t)_{y,x}$, or equivalently $\sum_{e,e'}(B^{t-1})_{e',e}\delta_{o(e),x}\delta_{t(e')=y}$.

In the sequel walks without back-scatter in which $e_{i+1} \neq \hat{e}_i,\ ,\ 1 \leq i \leq t-2$ will play an important rôle. We shall refer to them as *nb-walks* for short. To study nb-walks it is useful to define

$$J_{e,e'} = \delta_{\hat{e},e'}\ . \tag{3}$$

which singles out edges connected by backscatter. The matrix

$$Y = B - J \tag{4}$$

connects bonds which are not reversed. Thus, e.g., the number of t-periodic nb walks is $\mathrm{trY^t}$.

The probability that a long random walk visits any given vertex is completely controlled by the spectrum of the discrete Laplacian on the graph which is defined as

$$\Delta \equiv -A + dI^{(V)}, \tag{5}$$

where $I^{(V)}$ is the unit matrix in V dimensions. It is convenient to study the spectrum of A which differs from the Laplacian by a change of sign and a constant shift. The highest eigenvalue of A is d corresponding to a uniform distribution on the graph vertices. This implies that for d-regular graphs the limit distribution for a random walker is uniform (if the graph is connected and not bipartite). The distance between d and the next eigenvalue (the spectral gap $s(G)$) determines the speed at which a random walker covers the graph uniformly. For (V, d) regular graphs it is known [15] that the spectral gap is given asymptotically by

$$s(G) = d - 2\sqrt{d-1} + o\left(\frac{d}{\log V}\right) \tag{6}$$

with probability which converges to 1 exponentially fast in V. (Here and in the sequel, logarithms are calculated in base $d-1$). This result complements a previously established bound, [16]

$$s(G) < d - 2\sqrt{d-1} + \frac{2}{\log V}\ , \tag{7}$$

which implies that in the limit $V \to \infty$, the spectral gap cannot exceed $d - 2\sqrt{d-1}$. Hence, the limiting maximal mixing rate for regular graphs is attained asymptotically for almost any (V, d) graph. In other words, the d-regular graphs are optimal mixers. This strong mixing property is typical of hard classical chaos and it justifies the use of this model as a paradigm of quantum chaos as defined in the introduction.

Adjacency matrices of random d-regular graphs, have some remarkable spectral properties, which can be studied using the *spectral density* $\rho(\mu)$ and the *spectral counting function* $N(\mu)$ defined as :

$$\rho(\mu) \equiv \frac{1}{V} \sum_{\mu_a \in \sigma(A)} \delta(\mu - \mu_a) \quad ; \quad N(\mu) = V \int^{\mu} \mathrm{d}\rho(\mu) = \sum_{\mu_a \in \sigma(A)} \Theta(\mu - \mu_a) \ . \tag{8}$$

Here, μ_a are the adjacency eigenvalues corresponding to eigenvectors $f^{(a)} \in \mathbb{R}^V$.

An important discovery which marked the starting point of the study of spectral statistics for d-regular graphs was the derivation of the mean (in $\mathcal{G}(n,d)$) of the spectral density by Kesten [17] and McKay [18] :

$$\rho_{KM}(\mu) = \lim_{V\to\infty} \langle \rho(\mu) \rangle = \begin{cases} \frac{d}{2\pi} \frac{\sqrt{4(d-1)-\mu^2}}{d^2-\mu^2} & \text{for} \quad |\mu| \leq 2\sqrt{d-1} \\ \\ 0 & \text{for} \quad |\mu| > 2\sqrt{d-1} \end{cases} \ . \tag{9}$$

The proof of this result relies on the local tree property of random d-regular graphs, namely, that almost surely every subgraph of diameter less than $\log V$ is a tree. Counting periodic orbits on the tree can be done explicitly, and using the close relations between these numbers and the spectrum, one obtains (17). Note that the Kesten-Mckay density approaches Wigner's semi-circle law for large d.

A finite number of eigenvalues outside the support of ρ_{KM} cannot be excluded. Graphs for which the entire spectrum of A (except from the largest eigenvalue) lies within the support $[-2\sqrt{d-1}, 2\sqrt{d-1}]$, are called Ramanujan (For a review, see e.g., [19] and references cited therein). They are known to exist for some particular values of d, but much of their properties and their distribution are not known.

Finally, we shall consider the spectral properties of the "magnetic" Laplacian [20] which is defined in terms of the *magnetic adjacency matrix*

$$M_{i,j} = A_{i,j} \mathrm{e}^{i\phi_{i,j}} \ . \tag{10}$$

where the phases $\phi_{i,j}$ attached to the edges (i,j) play the rôle of "magnetic fluxes". The magnetic ensemble $\mathcal{G}^{(M)}(V,d)$ consists of $\mathcal{G}(V,d)$ augmented with independently and uniformly distributed phases $\phi_{i,j}$. In the following we shall use the superscript M consistently when referring to the magnetic ensemble. M is complex hermitian, and therefore the evolution it induces breaks time reversal symmetry. The largest eigenvalue of M may be different than d, but the asymptotic spectral density approaches the Kesten-Mackay distribution.

2 Spectral statistics and Trace formulae

One of the central themes in quantum chaos was the study of the statistics of spectral fluctuations. Analyzing the numerically computed spectral sequences of quantum billiards, led Bohigas, Giannoni and Schmit [21] to propose their conjecture : The spectral fluctuations for quantum chaotic systems follow the predictions of the Gaussian ensembles of Random Matrix Theory (RMT), while for integrable systems, they are Poissonian [22]. In the next paragraphs we shall review the numerical evidence which illustrates the excellent agreement between the spectral statistics

of the adjacency matrices of d-regular graphs (and their magnetic analogues) and the predictions of RMT [9, 6]. While describing these results a few concepts from RMT will be introduced [23].

2.1 Some numerical evidence and a few more definitions

For reasons which will become clear as the theory unfolds, it is advantageous to map the spectrum from the real line to the unit circle,

$$\phi_j = \arccos \frac{\mu_j}{2\sqrt{d-1}} \quad ; \quad 0 \leq \phi_j \leq \pi \ . \tag{11}$$

This change of variables is allowed since in the limit of large V, only a fraction of order $1/V$ of the spectrum is outside the support of the Kesten McKay distribution $[-2\sqrt{d-1}, 2\sqrt{d-1}]$ [25].

The mean (Kesten McKay) spectral density on the circle is not uniform,

$$\begin{aligned} \rho_{KM}(\phi) &= \frac{2(d-1)}{\pi d} \frac{\sin^2 \phi}{1 - \frac{4(d-1)}{d^2} \cos^2 \phi} \\ N_{KM}(\phi) &= V \frac{d}{2\pi} \left(\phi - \frac{d-2}{d} \arctan \left(\frac{d}{d-2} \tan \phi \right) \right) . \end{aligned} \tag{12}$$

Following the standard methods of spectral statistics, one introduces a new variable θ, which is uniformly distributed on the unit circle. This "unfolding" procedure is explicitly given by

$$\theta_j = \frac{2\pi}{V} N_{KM}(\phi_j) \tag{13}$$

The nearest spacing distribution defined as

$$P(s) = \lim_{V \to \infty} \ \frac{1}{V} \left\langle \sum_{j=1}^{V} \delta \left(s - \frac{V}{2\pi} (\theta_j - \theta_{j-1}) \right) \right\rangle \ , \tag{14}$$

is often used to test the agreement with the predictions of RMT (This was also the test conducted in ([9]). In this definition of the nearest spacing distribution, θ_0 coincides with θ_V, since the phases lie on the unit circle. In Fig. 1 we show numerical simulations obtained by averaging over 1000 randomly generated 3-regular graphs on 1000 vertices and their "magnetic" counterparts, together with the predictions of RMT for the COE and the CUE ensembles [24], respectively. The agreement is quite impressive.

Another quantity which is often used for the same purpose is the spectral form-factor,

$$K_V(t) = \frac{1}{V} \left\langle \left| \sum_{j=1}^{V} \mathrm{e}^{it\theta_j} \right|^2 \right\rangle \ . \tag{15}$$

The form-factor is the Fourier transform of the spectral two point correlation function and it plays a very important rôle in the understanding of the relation between RMT and the quantum spectra of classically chaotic systems [23, 28].

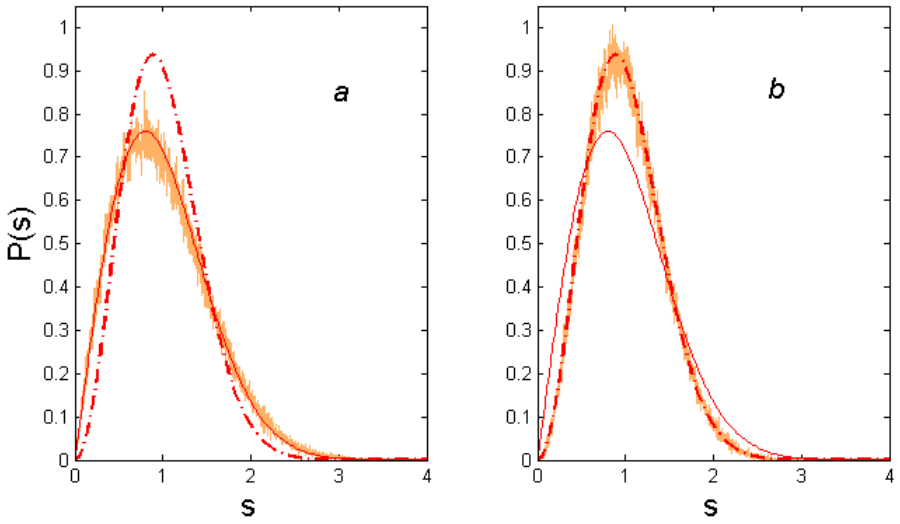

FIG. 1 – Nearest level spacings for : (a.) Graphs possessing time reversal symmetry. (b.) Magnetic graphs. Both figures are accompanied with the RMT predictions : Solid line - COE, Dashed line - CUE.

In RMT the form factor displays scaling : $\lim_{V\to\infty} K_V(t = \tau V) = K(\tau)$. The explicit limiting expressions for the COE and CUE ensembles are [24] :

$$K_{COE}(\tau) = \begin{cases} 2\tau - \tau\log(2\tau+1), & \text{for} \quad \tau < 1 \\ \\ 2 - \tau\log\frac{2\tau+1}{2\tau-1}, & \text{for} \quad \tau > 1 \end{cases} . \tag{16}$$

$$K_{CUE}(\tau) = \begin{cases} \tau, & \text{for} \quad \tau < 1 \\ \\ 1, & \text{for} \quad \tau > 1 \end{cases} . \tag{17}$$

The numerical data used to compute the nearest neighbor spacing distribution $P(s)$, was used to calculate the corresponding form factors for the non-magnetic and the magnetic graphs, as shown in Fig. 2. The agreement between the numerical results and the RMT predictions is apparent.

The above comparisons between the predictions of RMT and the spectral statistics of the eigenvalues of d-regular graphs was based on the unfolding of the phases ϕ_j into the uniformly distributed phases θ_j. As will become clear in the next sections, it is more natural to study here the fluctuations in the original spectrum and in particular the form factor

$$\widetilde{K}_V(t) = \frac{1}{V}\left\langle \left| \sum_{j=1}^{V} \mathrm{e}^{it\phi_j} \right|^2 \right\rangle . \tag{18}$$

The transformation between the two spectra was effected by (13) which is one-to-one and its inverse is defined :

$$\phi = S(\theta) \doteq N_{KM}^{-1}\left(V\frac{\theta}{2\pi}\right) . \tag{19}$$

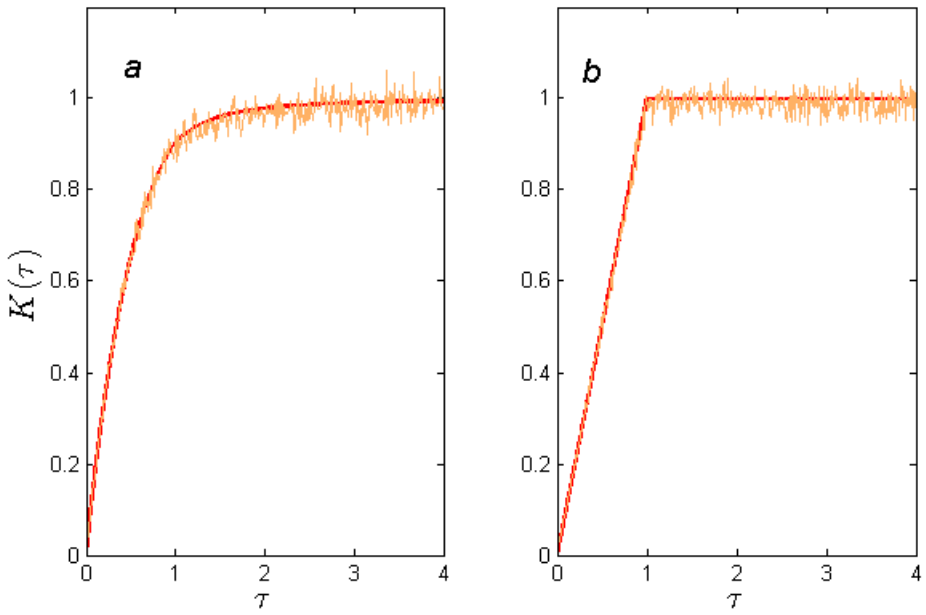

FIG. 2 – The form factor $K(\tau)$ (unfolded spectrum) for (a.) 3-regular graphs numerical *vs.* the COE prediction. (b.) 3-regular magnetic graphs *vs.* the CUE prediction.

This relationship enables us to express $\widetilde{K}_V(t)$ in terms of $K_V(t)$. In particular, if $K_V(t)$ scales by introducing $\tau = \frac{t}{V}$ then,

$$\widetilde{K}(\tau = \frac{t}{V}) = \frac{1}{\pi}\int_0^\pi d\theta K\left(\tau S^{'}(\theta)\right). \tag{20}$$

The derivation of this identity is straightforward. In the limit $\tau \to 0$, (20) reduces to

$$\widetilde{K}(\tau = \frac{t}{V}) \approx \frac{1}{2}K\left(\tau\right). \tag{21}$$

Fig. 3 shows $\widetilde{K}(\tau = \frac{t}{V}) = \widetilde{K}_V(t)$ computed by assuming that its unfolded analogue takes the RMT form (16) or (17), and it is compared with the numerical data for graphs with $d = 10$. It is not a surprise that this way of comparing between the predictions of RMT and the data, shows the same agreement as the one observed previously.

2.2 Trace formulae

The theoretical attempts to justify the Bohigas-Gianonni-Schmit conjecture were all based on *trace formulae* which establish a link between the quantum, spectral information, and the periodic manifolds in the phase-space of the underlying classical dynamics. The dichotomy observed in the quantum spectra is due to the intrinsic difference between the periodic manifolds in the corresponding classical dynamics : In chaotic systems the manifolds are discrete, unstable periodic orbits, while for integrable dynamics they correspond to periodic tori were the dynamics is

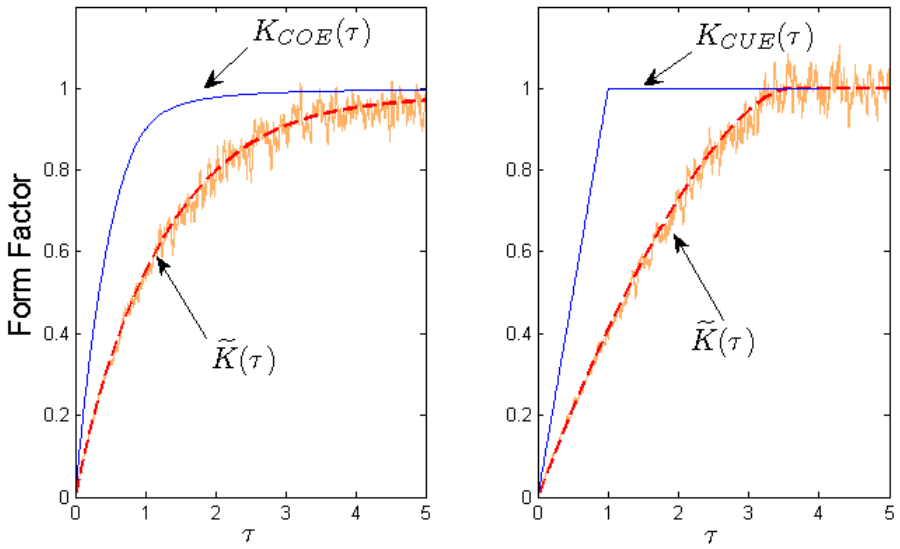

FIG. 3 – The form factor $\widetilde{K}(\tau)$ (original spectrum) for 10-regular graphs. The numerical results are presented *vs.* the expression (20) assuming RMT in the dashed line, and $K(\tau)$ (16), (17) in the solid line.

marginally stable. Trace formulae take the general form [27] :

$$\rho(E) \approx \rho_{smooth}(E) + \Im\left\{\sum_p A_p \mathrm{e}^{i(S_p(E)/\hbar + \frac{\pi}{2}\nu_p)}\right\} , \tag{22}$$

where E is the spectral parameter (Energy). ρ_{smooth} is a smooth function of E which provides the asymptotic behavior of $\rho(E)$. The sum is responsible to the oscillatory or fluctuating part of the spectral density. It goes over contributions from the periodic classical manifolds. The leading terms in the amplitudes A_p depend on the stability of the periodic orbits for chaotic billiards and on the phase space volume occupied by the corresponding torus for integrable cases. $S_p(E)$ are the action integrals along the periodic orbits and ν_p are the Maslov index which have a clear geometric meaning related to the orbit. The function which was most frequently studied in quantum chaos is the spectral 2-points correlation function :

$$R(\epsilon) = \frac{1}{\Delta}\int_{E_0-\Delta/2}^{E_0+\Delta/2} \tilde{\rho}(E+\epsilon/2)\tilde{\rho}((E-\epsilon/2)\mathrm{d}E \ , \quad \tilde{\rho}(E) = \rho(E) - \rho_{smooth}(E) \ , \tag{23}$$

or the *form-factor* which is its Fourier transform. Substituting the trace formula (22) in (23), one could express the spectral correlations in terms of correlations between classical actions [29]. The short time limit of the form factor predicted by RMT can be recovered by assuming that the actions of different periodic orbits are not correlated. (the "diagonal" approximation [28]). Further work elucidated the dynamical origin of the periodic orbit correlations [30]. This opened the way for a complete reconstruction of the RMT expression for the form factor based on the classical information and general symmetry considerations [31].

Following the quantum chaos example, the connection between spectral statistics and periodic orbit theory will be demonstrated by using trace formulae for

d-regular graphs.

We shall start by considering the spectrum of the adjacency matrices A. The trace formula can be obtained by making use of a well known identity [32, 33] which relates the characteristic polynomials and the spectra of the *vertex* adjacency matrix A and the *edge* nb-adjacency matrix Y (4) :

$$\det(I^{(2E)} - sY) = (1-s^2)^{E-V} \det(I^{(V)}(1+(d-1)s^2) - sA) \ . \tag{24}$$

For Ramanujan graphs, the spectrum consists of d and $|\mu_k| \leq 2\sqrt{d-1}$, $k = 1, \cdots (V-1)$. Transforming the μ_k to the unit circle as in (11), the spectrum of Y reads

$$\begin{aligned} \sigma(Y) \ &= \ \{(d-1), 1, \ +1 \times (E-V), \ -1 \times (E-V), \\ &\quad (\sqrt{d-1}\ \mathrm{e}^{i\phi_k}, \ \sqrt{d-1}\ \mathrm{e}^{-i\phi_k}, \ k = 1, \cdots (V-1))\Big\} . \end{aligned} \tag{25}$$

(The restriction to Ramanujan graphs can be removed [5] but this will not be discussed here). For large t, the number of t-periodic nb-walks given by $\mathrm{tr}Y^t$ is dominated by the largest eigenvalue, so that asymptotically $\mathrm{tr}Y^t \sim (d-1)^t$. It is advantageous to introduce

$$y_t^{(A)} = \frac{1}{V} \frac{\mathrm{tr}Y^t - (d-1)^t}{(\sqrt{d-1})^t} \tag{26}$$

which is the properly regularized number of t-periodic nb-walks. (The superscript (A) indicates reference to the spectrum of the adjacency matrix A) The explicit expressions for the eigenvalues of Y are used now to write,

$$y_t^{(A)} = \frac{1}{V}\left(\frac{1}{d-1}\right)^{\frac{t}{2}} + \frac{d-2}{2}\left(\frac{1}{d-1}\right)^{\frac{t}{2}} (1+(-1)^t) + \frac{2}{V}\sum_{k=1}^{V-1} \cos(t\phi_k) \ . \tag{27}$$

Multiplying by $\mathrm{e}^{it\phi}$ and summing one gets,

$$\rho(\phi) = \frac{2(d-1)}{\pi d} \frac{\sin^2\phi}{1 - \frac{4(d-1)}{d^2}\cos^2\phi} + \frac{1}{\pi} Re \sum_{t=3}^{\infty} y_t^{(A)} e^{it\phi} + \mathcal{O}\left(\frac{1}{V}\right) \ . \tag{28}$$

The first term is the smooth part, which is just the Kesten-McKay density. It is known from combinatorial graph theory that the counting statistics of t-periodic nb-walks with $t < \log V$ is Poissonian, with $\langle \mathrm{tr}Y^t \rangle = (d-1)^t$. Thus, the mean value of y_t vanishes as $\mathcal{O}\left(\frac{1}{V}\right)$. Hence, as expected,

$$\lim_{V\to\infty} \langle \rho(\mu) \rangle = \rho_{KM}(\mu). \tag{29}$$

The $O\left(\frac{1}{V}\right)$ correction to the smooth part is known explicitly but will not be quoted here. The trace formula (28) was derived previously by P. Mnëv, ([35]) in an entirely different way.

Equation (28) is the desired form of the trace formula. The summation extends over the contribution of t-periodic nb periodic walks, and the only information required for the spectral density are the $y_t^{(A)}$ - the normalized number of the periodic nb-walks. Note in passing that nb-walks appear in various contexts in combinatorial graph theory as in e.g.,[34]. Further comments on the trace formula are deferred to the last paragraphs in this chapter.

The trace formula for the spectrum of M has the same form. The only difference comes by replacing $y_t^{(A)}$ by :

$$y_t^{(M)} = \frac{1}{V} \frac{\sum_\alpha \mathrm{e}^{i\chi_\alpha}}{(\sqrt{(d-1)})^t} \quad , \tag{30}$$

where the sum above is over all the nb t-periodic walks, and χ_α is the total phase (net magnetic flux) accumulated along the t-periodic walk. For finite V, $\left\langle y_t^{(M)} \right\rangle \neq 0$ since $\chi_\alpha = 0$ for nb periodic walks where each bond is traversed equal number of times in the two directions. However, in the limit of large V, the number of such walks is small and therefore $\left\langle y_t^{(M)} \right\rangle \to 0$.

2.3 A periodic orbit expression for the spectral form-factor

Here and in the sequel, whenever the expression applies to both the A and M spectra, the superscripts (A) or (M) are deleted. Writing $\tilde{\rho}(\phi) = \rho(\phi) - \rho_{KM}(\phi)$ we get from the trace formula (28)

$$y_t = 2 \int_0^\pi \cos(t\phi)\tilde{\rho}(\phi) d\phi \ . \tag{31}$$

Thus,

$$\left\langle y_t^2 \right\rangle = 4 \int_0^\pi \int_0^\pi \cos(t\phi) \cos(t\psi) \left\langle \tilde{\rho}(\phi)\tilde{\rho}(\psi) \right\rangle d\phi d\psi \ . \tag{32}$$

Recalling (33)

$$\widetilde{K}_V(s) \equiv 2V \int_0^\pi \int_0^\pi \cos(s\phi) \cos(s\psi) \langle \tilde{\rho}(\phi)\tilde{\rho}(\psi) \rangle d\phi d\psi \ , \tag{33}$$

and comparing (32) and (33) we get :

$$\widetilde{K}_V(t) = \frac{V}{2} \left\langle y_t^2 \right\rangle \ . \tag{34}$$

So far the treatment of the two ensembles was carried on the same formal footing. We shall now address each ensemble separately.

2.3.1 The form factor for the $\mathcal{G}_{V,d}$ ensemble

In graph theory it is customary to discuss the number of nb t-cycles on the graph $C_t = \frac{Y_t}{2t}$ (in this definition, one does not distinguish between cycles which are conjugate to each other by time reversal). From combinatorial graph theory it is known that on average $\langle C_t \rangle = \frac{(d-1)^t}{2t}$ [36, 37, 38, 39]. Hence $\widetilde{K}$ can also be written as :

$$\widetilde{K}_V^{(A)}(t) = \frac{t}{V} \cdot \frac{\left\langle (C_t - \langle C_t \rangle)^2 \right\rangle}{\langle C_t \rangle} \ . \tag{35}$$

The expression of the spectral form factor $\widetilde{K}_V^{(A)}(t)$ in terms of combinatorial quantities is the main result of the present work. In particular, it shows that the form

factor is the ratio between the variance of C_t - the number of nb t-cycles - and its mean. This relation is valid for all t in the limit $V \to \infty$.

For t satisfying $t < logV$, it is known that asymptotically, for large V, the C_t's are distributed as independent Poisson variables. For a Poisson variable, the variance and mean are equal. Using (21) we get that for $\tau \ll 1$

$$K^{(A)}(\tau) = 2\tau \ . \tag{36}$$

This result coincides with the COE prediction (16). It provides the first rigorous support of the connection, established so far numerically, between RMT and the spectral statistics of graphs . It is analogous to Berry's "diagonal approximation" [28] in quantum chaos.

2.3.2 The form factor for the $\mathcal{G}^M_{V,d}$ ensemble

In the magnetic ensemble the matrices (10) are complex valued and Hermitian, which is tantamount to breaking time reversal symmetry. The relevant RMT ensemble in this case is the CUE.

In the ensuing derivation we shall take advantage of the statistical independence assumed for the magnetic phases which are uniformly distributed on the circle. Ensemble averaging will imply averaging over both the magnetic phases and the graphs.

Recall that $y_t^{(M)}$, in the case of magnetic graphs, was defined, by (30) :

$$y_t^{(M)} = \frac{1}{V} \frac{\sum_\alpha \mathrm{e}^{i\chi_\alpha}}{(\sqrt{(d-1)})^t} \ .$$

$y_t^{(M)}$ is the sum of interfering phase factors contributed by the individual nb t-periodic walks on the graph. The phase factors of periodic walks which are related by time reversal are complex conjugated. Periodic walks which are self tracing (meaning that every bond on the cycle is traversed the same number of times in both directions), have no phase : $\chi_\alpha = 0$. Using standard arguments from combinatorial graph theory one can show that for $t < \log_{d-1} V$, self tracing nb t-periodic walks are rare. Moreover, the number of t-periodic walks which are repetitions of shorter periodic walks can also be neglected. Hence

$$y_t^{(M)} \approx \frac{1}{V} \frac{2t \sum_\alpha{}' \cos(\chi_\alpha)}{(\sqrt{(d-1)})^t} \ . \tag{37}$$

where $\sum'$ includes summation over the nb t-cycles excluding self tracing and non-primitive cycles. The number of t-cycles on the graph is C_t, hence (37) has approximately C_t terms. From (37) and the definition of $y_t^{(M)}$, it is easily seen that $\langle (y_t^{(M)})^2 \rangle = \frac{1}{V^2(d-1)^t} 4t^2 \langle \left(\sum{}' \cos(\chi_\alpha) \right)^2 \rangle$. Averaging over the independent magnetic phases we get that

$$\widetilde{K}_V^{(M)}(t) = \frac{V}{2} \langle (y_t^{(M)})^2 \rangle \approx \frac{t}{2V} \equiv \frac{\tau}{2}. \tag{38}$$

For $\tau \to 0$, and using (21) we get

$$K^{(M)}(\tau) = \tau \ , \tag{39}$$

which agrees with the CUE prediction.

2.4 From RMT to combinatorial graph theory

We have shown above that by making use of the known asymptotic statistics of Y_t one can derive the leading term in the expansion of $K_V(t)$. It behaves as $g\tau$ where $g = 1, 2$ for the two graph ensembles, which is consistent with the predictions of RMT. Had we known more about the counting statistics, we could make further predictions and compare them to RMT results. However, to the best of our knowledge we have exhausted what is known from combinatorial graph theory, and the only way to proceed would be to take the reverse approach, and *assume* that the form factor for graphs is given by the predictions of RMT, and see what this implies for the counting statistics. Checking these predictions from the combinatorial point of view is beyond our scope. However, we shall show that they are accurately supported by the numerical simulations. In a way, this approach is similar to that of Keating and Snaith [40] who deduced the asymptotic behavior of the high moments of the Riemann ζ function on the critical line, by assuming that the Riemann zeros statistics follow the RMT predictions for the GUE ensemble.

The starting points for the discussion are the relations (34) and (20) which can be combined to give

$$\left\langle (y_t)^2 \right\rangle = \frac{2}{V}\widetilde{K}_V(t) = \frac{2}{V\pi}\int_0^\pi d\theta K\left(\tau S^{'}(\theta)\right) \ . \tag{40}$$

Our strategy here will be to use for the unfolded form factor the known expressions from RMT (16) and (17) and compute $\langle (y_t)^2 \rangle$. This will provide an expression for the combinatorial quantities defined for each of the graph ensembles, and expanding in τ we shall compute the leading correction to their known asymptotic values. The actual computations are somewhat cumbersome and will not be repeated here. Starting with the simpler CUE form we get for the $\mathcal{G}_M(V,d)$ assemblage,

$$\widetilde{K}^{(M)}(\tau) = \frac{\tau}{2} + f_1(d)\tau^{\frac{3}{2}} + \mathcal{O}\left(\tau^2\right) \tag{41}$$

where

$$f_1(d) = -\frac{1}{3\pi\sqrt{D}} \ \ ; \ \ D \equiv \frac{d(d-1)}{(d-2)^2} \ . \tag{42}$$

Thus, the difference $(\widetilde{K}^{(M)}(\tau) - \frac{\tau}{2})/f_1(d)$, should scale for small τ as $\tau^{\frac{3}{2}}$ for all values of d. This data collapse is shown in Fig. 4.

For the $\mathcal{G}(V,d)$ assemblage :

$$\widetilde{K}^{(A)}(\tau) = \tau + f_2(d)\tau^{\frac{3}{2}} + \dots \tag{43}$$

where

$$f_2(d) = \frac{1}{\sqrt{2D}}\left(\frac{2}{\pi}\cdot \mathrm{arccoth}(\sqrt{2}) - \frac{2\sqrt{2}}{3\pi} - 1\right). \tag{44}$$

Thus, the difference $(\widetilde{K}^{(A)}(\tau) - \tau)/f_2(d)$, at small τ, should scale as $\tau^{\frac{3}{2}}$ independently of d. This data collapse is shown in Fig. 5.

Using the above and (35) we can write,

$$\frac{\left\langle (C_t - \langle C_t \rangle)^2 \right\rangle}{\langle C_t \rangle} = \frac{1}{\tau\pi}\int_0^\pi d\theta K_{COE}\left(\tau S^{'}(\theta)\right) \underset{\tau\to 0}{\longrightarrow} 1 + f_2(d)\sqrt{\tau} + \dots \tag{45}$$

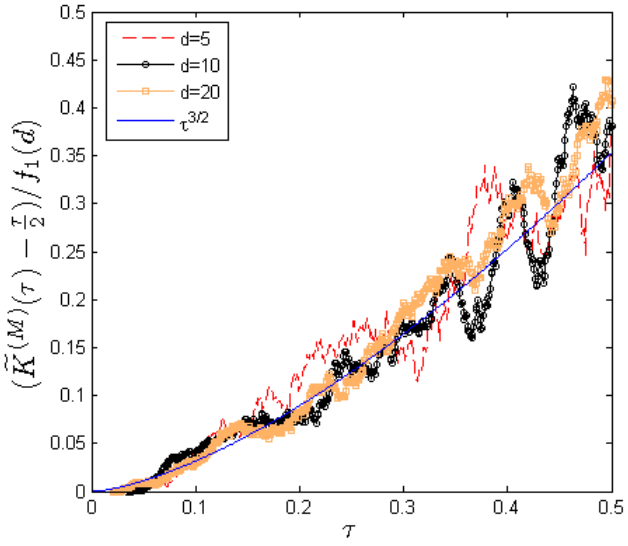

FIG. 4 – $(\widetilde{K}^{(M)}(\tau)-\frac{\tau}{2})/f_1(d)$ for various values of d *vs.* the curve $\tau^{\frac{3}{2}}$.

If the C_t's were Poissonian random variables, the expansion above would terminate at 1. Since it does not, we must conclude that the C_t's are not Poissonian. The highest order deviation comes from the next order term in the expansion which is proportional to $\tau^{\frac{1}{2}}$. The coefficient, $f_2(d)$, is explicitly calculated above.

We can examine the behavior at another domain of τ, namely $\tau > 1$. It can easily be shown that $S'(\theta) \geq \frac{d}{4(d-1)}$. Consequently, for $\tau > \frac{4(d-1)}{d}$, the argument of K in (20) is larger than one, and so

$$\lim_{\tau\to\infty} \widetilde{K}^{(A)}(\tau) = 1. \tag{46}$$

Combining this result with (35), provides the asymptotic of the variance-to-mean ratio :

$$\lim_{\tau\to\infty} \tau \frac{var(C_t)}{\langle C_t\rangle} = 1, \quad \text{for } V,t\to\infty; \quad \frac{t}{V} = \tau \tag{47}$$

This is a new interesting combinatorial result, since very little is known about the counting statistics of periodic orbits in the regime of $\tau > 1$.

2.5 Some comments on trace formulae

The trace formula quoted in (28) is but a single expression taken from a continuum of formulae, all of them are exact, pertain to the same spectral density, but make use of a different class of periodic orbits. For every real parameter $w \in [1, \frac{d-1}{2}]$, and $d \geq 3$ one can write a trace formula for the spectrum of the adjacency matrix. Writing the spectral density in terms of the spectral parameter μ the trace assumes the standard separation between the smooth and the oscillatory part :

$$\rho(\mu) = \rho_{smooth}(\mu; w) + \tilde{\rho}(\mu; w) + \mathcal{O}\left(\frac{1}{V}\right). \tag{48}$$

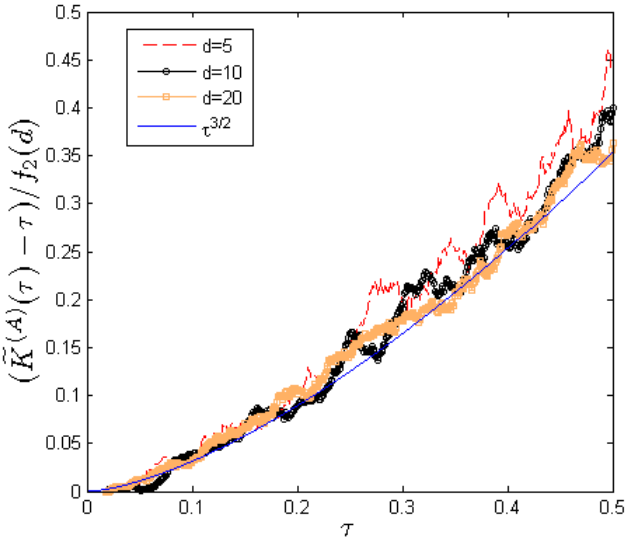

FIG. 5 – $(\widetilde{K}^{(A)}(\tau)-\tau)/f_2(d)$ for various values of d *vs.* the curve $\tau^{\frac{3}{2}}$.

Here, however, the expression for the smooth part

$$\rho_{smooth}(\mu;w) = \frac{d/(2\pi)}{\sqrt{4w(d-w)-\mu^2}}\left(1-\frac{(d-2w)(d-2)}{d^2-\mu^2}+\frac{(w-1)^2(\mu^2-2w(d-w))}{w^2(d-w)^2}\right) \quad (49)$$

differs from the Kesten-McKay expression. In other words, when both sides of (48) are averaged over the ensemble, $\langle\tilde{\rho}(\mu,w)\rangle \neq 0$! The oscillatory part takes the form,

$$\tilde{\rho}(\mu;w) = \frac{1}{\pi}\mathcal{R}e\left(\sum_{t=3}^{\infty}\frac{y_t(w)}{\sqrt{4w(d-w)-\mu^2}}\exp^{it\frac{\mu}{2\sqrt{w(d-w)}}}\right) . \quad (50)$$

The information about the periodic walks is stored in $y_t(w)$ (the analogue of y_t above (26)). Here, *all the t-periodic walks* are contributing, and every backscatter is endowed with a weight $(1-w)$. Denting by $N(t;g)$ the number of t-periodic walks which backscatter exactly g times, $y_t(w)$ is

$$y_t(w) = \frac{1}{V}\frac{\sum_g N(t;g)(1-w)^g-(d-w)^t}{(\sqrt{w(d-w)})^t} . \quad (51)$$

Each of the two terms which contribute to $\rho(\mu)$ depend on w yet, their sum does not. The dependence of $\tilde{\rho}(\mu;w)$ on w comes from two sources - the weights of the backscattered orbits and the phase factor. Hence, the re-summation required to obtain (28) which corresponds to $w=1$ from (50) with $w\neq 1$ is far from being trivial. Exploratory studies [5] show how combinatorial expressions for counting certain families of periodic walks can be derived by studying the w dependence of the trace formula. Reviewing this study exceeds the scope of the present review, and it is mentioned only to indicate the potential wealth stored in this and other parametric dependent trace formulae. Another family of trace formula was written down in [4], but will not be discussed here.

3 Eigenfunctions

There are several interesting properties which mark the eigenfunctions of the Schrödinger operator in quantum chaotic systems. The most frequently studied models are quantum chaotic billiard domains $\Omega \in \mathbb{R}^2$, and their properties will serve as a bench-mark for the comparison with the properties of eigenvectors of the adjacency matrices A corresponding to d-regular graphs.

The most important features displayed by wave-functions of quantum chaotic billiards are :

– Almost all eigenfunctions ψ_n (ordered by increasing value of the spectral parameter and square normalized) for sufficiently large n, are distributed uniformly in the sense that given any smooth "observable" $A(x),\ x \in \Omega$

$$\int_\Omega \psi_n^2(x) A(x) \mathrm{d}^2 x \to \int_\Omega A(x) \mathrm{d}^2 x \tag{52}$$

when $n \to \infty$ on all integer sequences from which sequences of zero measure might be excluded. [41]

– On the atypical sequences, the eigenfunction might show high concentration near classically periodic orbits - a phenomenon known as scarring [42].

– In the limit of large n, the wave functions are conjectured to behave in probability as uniformly distributed Gaussian variables with the covariance

$$\langle \psi_n(x) \psi_n(y) \rangle = J_0(k_n |x - y|) \ . \tag{53}$$

Here, the triangular brackets stand for an average over a properly defined spectral interval about the mean eigenvalue k_n^2. The points x, y are in the billiard domain and sufficiently remoted from the boundaries, and $J_0(x)$ is the Bessel function of order 0. While the statement that the distribution is Gaussian is not proven rigorously, it is supported by numerical simulations, the correlation function can be justified in the semi-classical limit. This property is sometimes refer to as the random wave model [43].

– The nodal domains (defined as the connected domains where $\psi_n(x)$ have a constant sign) in quantum chaotic billiards display two features - their normalized count $\frac{\nu_n}{n}$ narrowly distribute around a universal number. Moreover, they cover Ω in patterns typical to critical percolation. [21, 46]

Back to d-regular graphs : The local tree property of d-regular graphs is at the basis of our present understanding of the statistical properties of the adjacency eigenvectors. Considering the infinite d-regular tree, Y. Elon [2] was recently able to properly construct a "random wave" model on the infinite d-regular tree whose Gaussian distribution can be rigorously assessed. The covariance for the Gaussian field is

$$\begin{aligned} \phi^{(\lambda)}(s) &\doteq \langle f_i f_j \rangle = (d-1)^{-s/2} \left(\frac{d-1}{d} U_s \left(\tfrac{\lambda}{2\sqrt{d-1}} \right) - \frac{1}{d} U_{s-2} \left(\tfrac{\lambda}{2\sqrt{d-1}} \right) \right) \\ s &= |i - j| \ . \end{aligned} \tag{54}$$

Here, $f_i(\lambda)$ stands for the component of the adjacency eigenvector at the vertex i, with the normalization $\langle f_i^2 \rangle = 1$. The distance $s = |i - j|$ on the graph is the length of the minimal walk between the vertices i, j, $U_k(x)$ are the Chebyshev polynomials of the second kind, and the triangular brackets denote averaging over the

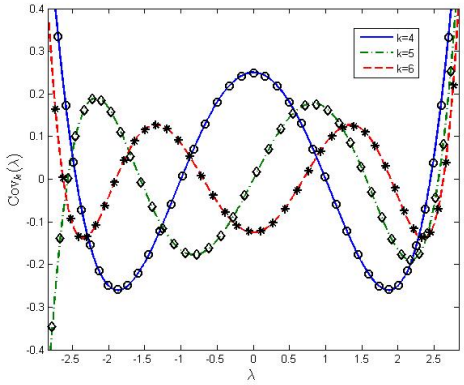

FIG. 6 – A comparison between (54)(marked by lines), and the numerical covariance, for a single realization of $G(4000, 3)$ (denoted by different symbols), where $\log_{d-1}(n) = 11.97$, for $k = 4, 5, 6$ (the local tree regime).

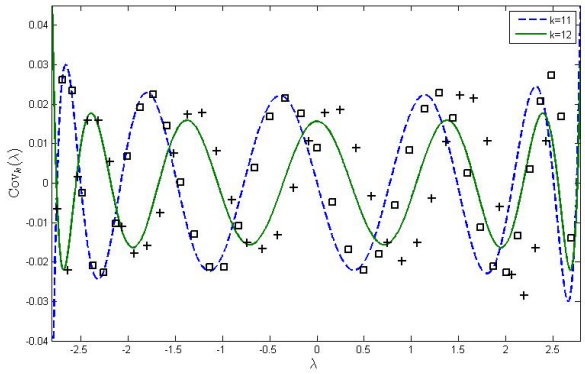

FIG. 7 – A comparison between (54) (marked by lines), and and the numerical covariance, for $G(4000, 3)$ and $k = 11, 12$ (beyond the tree regime).

random wave ensemble. Taking into account the asymptotic behavior of the Chebyshev polynomials, one can recognize (54) as the analogue of the correlation function of random waves for planar random waves (53).

Due to the local tree property, it is natural to expect, (but not yet rigorously proved), that in the limit $V \to \infty$ the properties derived for the tree graph, will also hold for $\mathcal{G}(V, d)$, for distances within the range $s \leq \log V$. This was tested numerically, and the (multivariate) Gaussian distribution for the components of the adjacency eigenvectors was checked within the numerical accuracy. Figs. 6. and 7. summarize the numerical tests.

As in billiards, one can define nodal domains of the adjacency vectors as the connected sub-graphs where the eigenvector components have a constant sign. The number of nodal domains obeys the analogue of Courant theorem [44]. There is no known way to count nodal domains in billiards or even in arbitrary graphs. Y. Elon [1] proposed recently a method to compute the expected number of nodal domains in d-regular graphs as a function of the corresponding eignevalue. His argument will be sketched here.

For a graph G and an adjacency eigenvector $f(\lambda)$, the *induced nodal graph* $\tilde{G}_f$

is obtained by the deletion of edges, which connect vertices that possess opposite signs in f

$$\tilde{G}_f = (V, \tilde{E}_f) \quad , \quad \tilde{E}_f = \{(v_i, v_j) \in E | f_i f_j > 0\} \tag{55}$$

We also define

$$p_e(f(\lambda)) = \mathbb{P}(e \in \tilde{E}_f) \tag{56}$$

to denote the probability that a random edge $e \in E$ survives the nodal trimming. According to the random waves hypothesis, $p_e(f(\lambda))$ should typically converge as $V \to \infty$ into

$$\begin{aligned} p_e(\lambda) &= 2\int_0^\infty \int_0^\infty d\mathbf{f} \frac{1}{2\pi\sqrt{|\mathcal{C}_\lambda|}} \exp\left(-\frac{1}{2}\langle \mathbf{f}, \mathcal{C}_\lambda^{-1}\mathbf{f}\rangle\right) \\ &= \frac{1}{2} + \frac{1}{\pi}\arcsin\left(\frac{\lambda}{d}\right) \end{aligned} \tag{57}$$

where $\mathbf{f} = (f_1, f_2)$ and the covariance operator elements are $(\mathcal{C}_\lambda)_{11} = (\mathcal{C}_\lambda)_{22} = \phi^{(\lambda)}(0) = 1$, $(\mathcal{C}_\lambda)_{12} = (\mathcal{C}_\lambda)_{21} = \phi^{(\lambda)}(1) = \lambda/d$. ($\phi^{(\lambda)}(s)$ is the covariance defined in (54)). This results which follows from the random waves conjecture was checked numerically and found to reproduce the simulations in a perfect way.

Since on average, the induced nodal graph $\tilde{G}_f$ posses $p_e(\lambda)\cdot|E| = \frac{nd}{2}p_e(\lambda)$ edges and V vertices, the expected nodal count may be bounded from below (for all of the eigenvectors but the first) by neglecting the cycles in $\tilde{G}$:

$$\mathbb{E}\left(\frac{\nu(\lambda)}{V}\right) \geq \max\left\{\frac{2}{V}, \left(1 - \frac{d}{2}p_e(\lambda)\right)\right\} \tag{58}$$

While (58) lose its efficiency as d increases[1], for low values of d, this crude bound matches surprisingly well the observed nodal count as shown in Fig. 8. By taking

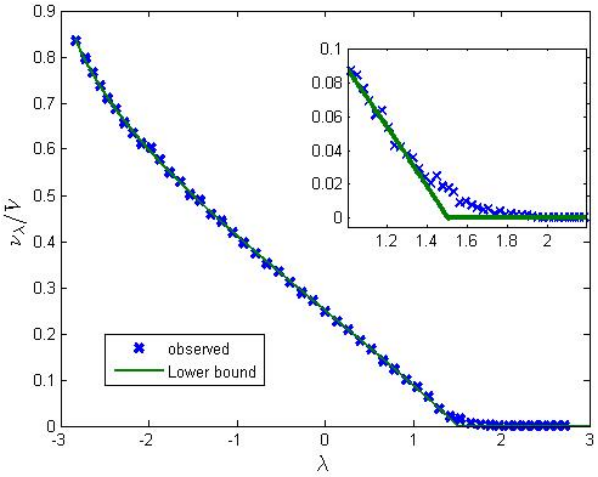

FIG. 8 – A comparison between the theoretical estimate for the nodal count and the observed count for a single realization of $G(4000, 3)$. The inset is a magnification of the spectral window near the bound's flexion - the only part of the spectrum, in which the observed count deviates considerably from the bound.

[1]In fact, for $d > 7$, $\forall\lambda, 1 - dp_e(\lambda)/2 < 0$. Therefore tn that case the bound becomes trivial.

into account more correlations, Elon was able to improve the crude bound above [1]. Due to space limitation this will not be discussed here any further.

Percolation is an important topic of research in probabilistic graph theory [47]. This subject was recently extended [3] by defining percolation of level sets of the adjacency eigenvectors as explained below. The α level set of an eigenvector is defined as the subgraph where $\tilde{G}_\alpha = \{v_i \in G : f_i > \alpha\}$ (the normalization $\frac{1}{V}\sum_i f_i^2 = 1$ is assumed). Given an adjacency eigenvector (corresponding to an eigenvalue λ) one can study the α dependence of the ratio

$$\frac{|\tilde{G}_\alpha^{max}|}{|\tilde{G}_\alpha|} \tag{59}$$

where $\tilde{G}_\alpha^{max}$ is the maximal connected component in $\tilde{G}_\alpha$. The α level set will be called percolating once $\tilde{G}_\alpha^{max} \sim V$. A percolation transition occurs at $\alpha_c(\lambda)$ if, in the limit $V \to \infty$ and for almost all graphs in $\mathcal{G}(V,d)$, the ratio (59) is discontinuous at $\alpha = \alpha_c(\lambda)$. The transition for a single large graph is shown in Fig. (9) for a few values of λ. Assuming the validity of the random wave conjecture, Y. Elon was able

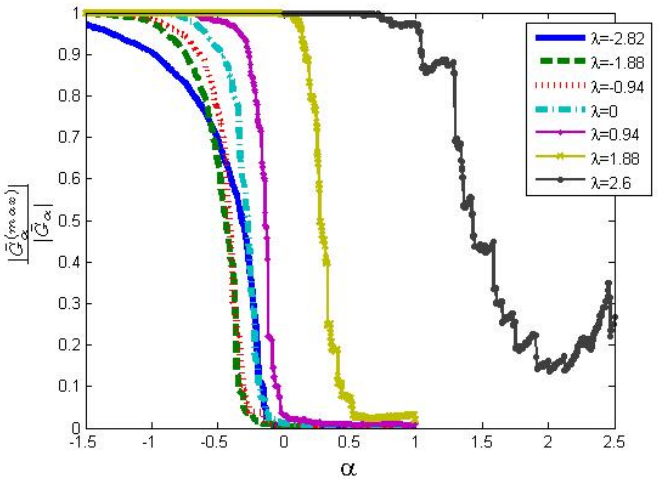

FIG. 9 – The ratio between the magnitude of the largest level set to the size of the induced graph $\tilde{G}_\alpha$ for a single realization of a $(4000, 3)$ graph. each curve corresponds to one eigenvector, while α is varied along the curve.

to compute the dependence of the critical level on both λ and d, and found a very good agreement with the numerical results, as shown in Fig. 10

The applicability of the random wave conjecture of the adjacency vectors is supported very robustly by the numerical and theoretical considerations. A rigorous validation is still lacking.

4 Scattering

Chaos is usually associated with bounded dynamical systems. However, classical chaos can be defined and studied also in open (scattering) systems, and its quantum analogue provided many interesting theoretical problems and practical applications [48, 49, 50]. In this section, it will be shown how a bound finite graph

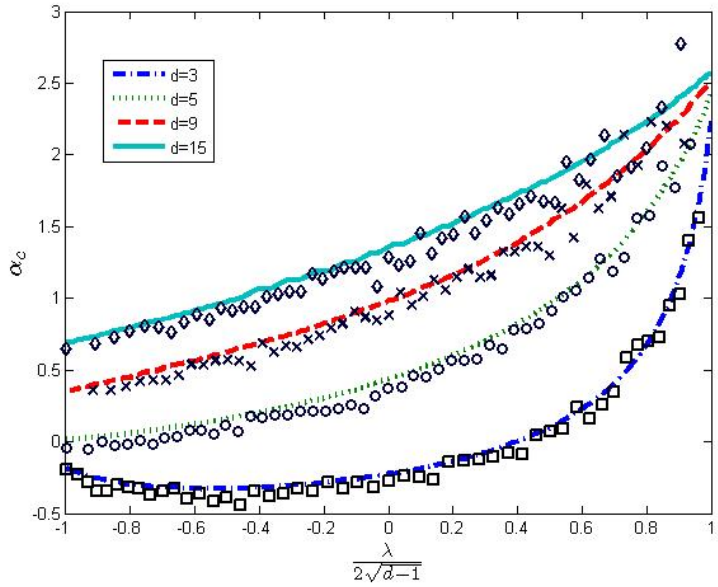

FIG. 10 – A comparison between the theoretical estimates of $\alpha_c(\lambda, d)$ based on the random wave model (lines) to the numerically computed $\alpha_c(\lambda, d)$ for (V, d) graphs (markers).

can be converted to a scattering system by attaching "leads" to infinity [7, 51]. An expression for the scattering matrix will be provided, which can be further studied in various contexts such as e.g., resonance distribution and conductance fluctuations and correlations.

Consider a finite (not necessarily d-regular) graph $\mathcal{G}^{(0)}$. In what follows, all quantities belonging to $\mathcal{G}^{(0)}$ will be denoted by a superscript (0). In particular, $D_i^{(0)}$ stands for the degree of the vertex i in $\mathcal{G}^{(0)}$. Scattering is defined by attaching to any subset of the vertices lead graphs which are defined as follows : A lead graph l is a semi-infinite set of vertices $(l,1),(l,2),\cdots$ which are connected linearly. A vertex is identified by a double index (l,i), l denotes the lead, and i enumerates the vertex position on the lead. The lead connectivity (adjacency) matrix is $A^{(Lead)}_{(l,n),(l',n')} = w\delta_{l,l'}\delta_{|n-n'|,1}$, $n, n' \in \mathbb{N}^+$, where w stands for the number of parallel bonds which connect successive vertices. (All quantities related to the leads will be denoted by the superscript $(Lead)$). The spectrum of the lead Laplacian $\Delta_l^{(Lead)}$ and the corresponding eigenfunctions $\mathbf{f} = \left(f_{(l,1)}, f_{(l,2)}, \cdots\right)^\top$ satisfy

$$\begin{aligned}(\Delta_l^{(Lead)}\mathbf{f})_{(l,n)} &= -w(f_{(l,n+1)} + f_{(l,n-1)}) + 2wf_{(l,n)} = \lambda f_{(l,n)} \quad \text{for } n > 1 \ , \\ &= -wf_{(l,2)} \qquad + \qquad wf_{(l,1)} = \lambda f_{(l,1)} \quad \text{for } n = 1 \ . \end{aligned} \tag{60}$$

The spectrum is continuous and supported on the spectral band $\lambda \in [0, 4w]$ (the conduction band). For any λ in the conduction band, there correspond two eigenfunctions which can be written as linear combinations of counter-propagating waves :

$$f^{(\pm)}_{(l,n)} = \xi_\pm^{n-1} \quad \text{where} \quad \xi_\pm = 1 - \frac{\lambda}{2w} \pm \sqrt{\left(1 - \frac{\lambda}{2w}\right)^2 - 1} = \mathrm{e}^{\pm i\alpha(\lambda)} \ . \tag{61}$$

For $\lambda > 4w$, $|\xi_-| > |\xi_+|$. The reason for constructing the leads with w parallel bonds is because the conduction band can be made arbitrarily broad. In the present application, an appropriate choice of w would be of the order of the mean valency in the interior graph, so the spectrum of $\mathcal{G}^{(0)}$ falls well within the conduction band.

A function which satisfies the boundary condition at $n = 1$ (second line of (60)) is,

$$f_{(l,n)} = f^{(-)}_{(l,n)} + s_l(\lambda) f^{(+)}_{(l,n)} \ , \tag{62}$$

where

$$s_l(\lambda) = -\frac{1-\xi_+}{1-\xi_-} \ = \xi_+ \quad , \quad |s_l(\lambda)| = 1 \text{ for } \lambda \in [0, 4w] \ . \tag{63}$$

The lead scattering amplitude $s_l(\lambda)$ provides the phase gained by scattering at the end of the lead (as long as λ is in the conduction band).

Returning now to the interior graph $\mathcal{G}^{(0)}$ it is converted into a scattering graph by attaching to its vertices semi-infinite leads. At most one lead can be attached to a vertex, but not all vertices should be connected to leads. Let $\mathcal{L}$ denote the set of leads, and $L = |\mathcal{L}|$. The connection of the leads to $\mathcal{G}^{(0)}$ is given by the $V^{(0)} \times L$ "wiring" matrix

$$W_{j,(l,1)} = \begin{cases} 1 & \text{if } j \in \mathcal{V}^{(0)} \text{ is connected to } l \in \mathcal{L} \\ 0 & \text{otherwise} \end{cases} \quad . \tag{64}$$

The number of leads which emanate from the vertex i is either 0 or 1, and is denoted by $d_i = W_{i,(l,1)}$. Define also the diagonal matrix $\tilde{D} = \mathrm{diag}(d_i)$ so that

$$W W^\top = \tilde{D} \quad ; \quad W^\top W = I^{(L)} \ , \tag{65}$$

where $I^{(L)}$ is the $L \times L$ unit matrix.

The scattering graph $\mathcal{G}$ is the union of $\mathcal{G}^{(0)}$ and the set of leads $\mathcal{L}$. Its vertex set is denoted by $\mathcal{V}$ and its adjacency matrix A for $\mathcal{G}$ is given by,

$$\forall i,j \in \mathcal{V}, \ : \quad A_{i,j} = \begin{cases} A^{(0)}_{i,j} & \text{if } i,j \in \mathcal{V}^{(0)} \\ A^{(Lead)}_{i=(l,i),j=(l,j)} & \text{if } l \in \mathcal{L} \\ w W_{i,j=(l,1)} & \text{if } i \ \in \mathcal{V}^{(0)} \text{ and } l \in \mathcal{L} \end{cases} \quad . \tag{66}$$

As is usually done in scattering theory, one attempts to find eigenfunctions $\mathbf{f}$ of the discrete Laplacian of the scattering graph, subject to the condition that on the leads $l = 1, \cdots, L$ the wave function consists of counter propagating waves :

$$f_{(l,n)} = a_l \xi_-^{n-1} + b_l \xi_+^{n-1} \ , \ n \ \geq \ 1 \ . \tag{67}$$

where a_l and b_l are the incoming and outgoing amplitudes. They are to be determined from the requirement that $\mathbf{f}$ is an eigenfunction of the scattering graph Laplacian. It will be shown below that this requirement suffices to provide a linear relationship between the incoming and outgoing amplitude. The $L \times L$ scattering matrix $S^{(Lead)}(\lambda)$ is defined as the mapping from the incoming to the outgoing amplitudes :

$$\mathbf{b} = S^{(Lead)}(\lambda) \mathbf{a} \ . \tag{68}$$

To compute $S^{(Lead)}(\lambda)$, consider the action of the Laplacian on an eigenvector $\mathbf{f}$.

$$\begin{aligned}
\forall i \in \mathcal{V}^{(0)} : (\Delta\mathbf{f})_i &= -\sum_{j\in\mathcal{V}^{(0)}} A^{(0)}_{i,j} f_j - w\sum_{l\in\mathcal{L}} W_{i,(l,1)} f_{(l,1)} + (D^{(0)}_i + wd_i) f_i = \lambda f_i. \\
\forall l \in \mathcal{L} : (\Delta\mathbf{f})_{(l,1)} &= -w\sum_{i\in\mathcal{V}^{(0)}} W^{\top}_{(l,1),i} f_i - w f_{(l,2)} + 2w f_{(l,1)} = \lambda f_{(l,1)} \ . \\
(\Delta\mathbf{f})_{(l,n)} &= -w f_{(l,n+1)} - w f_{(l,n-1)} + 2w f_{(l,n)} = \lambda f_{(l,n)}. \qquad (69)
\end{aligned}$$

The equations for $i \in \mathcal{V}^{(0)}$ (first line in (69) above), can be put in a concise form :

$$\left(\Delta^{(0)} + w\tilde{D} - \lambda I^{(V^{(0)})}\right)\mathbf{f}^{(V^{(0)})} = wW\mathbf{f}_1^{(L)} \ . \qquad (70)$$

where $I^{(V^{(0)})}$ is the unit matrix in $V^{(0)}$ dimension, $\mathbf{f}^{(V^{(0)})}$ is the restrictions of $\mathbf{f}$ to the vertices of the interior graph $\mathcal{G}^{(0)}$ and $\mathbf{f}_1^{(L)}$ is the L dimensional vector with components $f_{(l,1)},\ l = 1, \cdots, L$. For λ away from the eigenvalues of $\Delta^{(0)} + w\tilde{D}$ the $V^{(0)} \times V^{(0)}$ matrix $R^{(0)}(\lambda)$ is defined as,

$$R^{(0)}(\lambda) = \left(\Delta^{(0)} + w\tilde{D} - \lambda I^{(V^{(0)})}\right)^{-1} \ . \qquad (71)$$

Thus,

$$\mathbf{f}^{(V^{(0)})} = wR^{(0)}W\mathbf{f}_1^{(L)} \ . \qquad (72)$$

Substituting in the second set of equations in (69) and using (67),

$$\left(-w^2 W^{\top} R^{(0)}(\lambda) W + (2w - \lambda) I^{(L)}\right)(\mathbf{a} + \mathbf{b}) = w(\mathbf{a}\ \xi_- + \mathbf{b}\ \xi_+). \qquad (73)$$

This can be easily brought into the form (68). Using the fact that $2 - \lambda/w = \xi_- + \xi_+$ we get,

$$S^{(Lead)}(\lambda) = -\left(wW^{\top}R^{(0)}(\lambda)W - \xi_-\ I^{(L)}\right)^{-1}\left(wW^{\top}R^{(0)}(\lambda)W - \xi_+\ I^{(L)}\right) \ . \qquad (74)$$

This is the desired form of the scattering matrix. It has a few important properties. *i.* As long as λ is in the conduction band, ξ_- and ξ_+ are complex conjugate and unitary. Since $W^{\top}R^{(0)}(\lambda)W$ is a symmetric real matrix, $S^{(Lead)}(\lambda)^{\top} = S^{(Lead)}(\lambda)$ and $S^{(Lead)}(\lambda)S^{(Lead)}(\lambda)^{\dagger} = I^{(L)}$, that is, $S^{(Lead)}(\lambda)$ is a symmetric and unitary matrix.
ii. Once λ is outside of the conduction band, the $f^{(\pm)}_{(l,n)}$ are exponentially increasing or decreasing solutions - they are the analogues of the evanescent waves encountered in the study of wave-guides. One of the reason for the introduction of the w parallel bonds in the leads was to broaden the conduction band and avoid the spectral domain of evanescent waves. However, for the sake of completeness one observes that the scattering matrix as defined above can be analytically continued outside of the conduction band by using (61) which is valid for any λ. The $S^{(Lead)}(\lambda)$ matrix outside the conduction band loses its physical interpretation, and it remains symmetric but is not any more unitary. However, it is a well defined object, and can be used in the sequel for any real or complex λ. In the limit $\lambda \to \infty$, $S^{(Lead)}(\lambda) \to \xi_+ W^{\top}R^{(0)}(\lambda)W \approx \left(\frac{w}{\lambda}\right)^2 I^{(L)}$.
iii. At the edges of the conduction band $\xi_\pm(\lambda = 0) = 1\ ;\ \xi_\pm(\lambda = 4w) = -1$. Substituting in (74) one finds that at the band edges, $S^{(Lead)} = -I^{(L)}$.

iv. The matrix $R^{(0)}(\lambda)$ is well defined for λ away from the spectrum of $\Delta^{(0)} + w\tilde{D}$. Approaching these values does not cause any problem in the definition of $S^{(Lead)}(\lambda)$ since there $S^{(Lead)} = -I^{(L)}$. However, for sufficiently large w the singularities of $R^{(0)}(\lambda)$ can be separated away from the domain where the spectrum of $\mathcal{G}^{(0)}$ is supported.
v. The resonances are defined as the poles of the scattering matrix in the complex λ plane. They are the solution of the equation

$$z_{res}(\lambda) = \det\left(wW^{\top}R^{(0)}(\lambda)W - \xi_{-}\ I^{(L)}\right) = 0\ . \tag{75}$$

The point $\lambda = 0$ is not a pole since $S^{(Lead)}(\lambda = 0) = -I^{(L)}$.
vi. Finally, it might be instructive to note that the matrix $R^{(0)}(\lambda)$ is closely related to the discrete analogue of the Dirichlet to Neumann map. This can be deduced from the following construction : add to each vertex $i \in \mathcal{V}^{(0)}$ a new auxiliary vertex $\tilde{i}$ connected exclusively to i. (Here we use $w = 1$ to make the analogy clearer). Write the discrete Laplacian for the new graph, and solve $(\Delta - \lambda I)\tilde{\mathbf{f}} = 0$, where $\tilde{\mathbf{f}}$ is a $2V^{(0)}$ dimensional vector, the first V entries correspond to the original vertices, and the last V entries correspond to the auxiliary vertices : $\tilde{\mathbf{f}} = (\mathbf{f}, \mathbf{g})^{\top}$. Assuming that the values $g_{\tilde{i}}$ on the auxiliary vertices are given, the entries in $\mathbf{f}$ can be expressed as $\mathbf{f} = R(\lambda)\mathbf{g}$, where $R(\lambda)$ as defined in (71). To emphasize the connection to the Dirichlet to Neumann map, define $\psi = \frac{1}{2}(\mathbf{g} + \mathbf{f})$ (the "boundary function") and $\partial\psi = (\mathbf{g} - \mathbf{f})$ (the "normal derivative") then,

$$\partial\psi = M(\lambda)\psi \quad ; \quad M(\lambda) = 2(I^{(V^{(0)})} + R(\lambda))^{-1}(I^{(V^{(0)})} - R(\lambda))\ . \tag{76}$$

The Dirichlet to Neumann map is defined also in other applications of graph theory, see e.g., [52].

The general setup displayed above can be easily converted to the case of d-regular graphs, and the information accumulated for their spectral and eigenfunctions properties could be used in the scattering context. This program is now under study.

5 Summary and prospects

The three topics covered in the preceding sections are at the center of the research in quantum chaos, and the close conceptual and technical links with quantum chaos substantiate the claim expressed by the title of the present article - indeed, d-regular graphs are a paradigm model for quantum chaos. This model is as rich as the "quantum graphs" which where introduced a while ago, and turned out to be a very fertile domain in its own right, and provided several new insights to problems which are commonly addressed in "quantum chaos". [53, 54, 55] As much of the research reported here is the result of work done in the past three years only, much remains to be done, and a few routes should be opened to explore further the potential stored in the d-regular graphs model.
i. The connection between graph combinatorics and spectral statistics should go much more deeply than what is known today. As was shown above, this research at the interface of the two fields stores potential advantages in both directions.
ii. Isospectral d-regular graphs are known to exist [56], and methods to build them systematically were proposed by several authors. It was suggested some time ago that

the nodal domain counts can be used to distinguish between isospectral domains. Some analytical results on small and simple graphs, and numerical simulations pertaining for large graphs support the validity of this conjecture. Further research is needed to substantiate these claims in a rigorous way.
iii. The range of the graph model can be extended in a major way by assigning weights to the edges, and / or potentials to the vertices. The graph Laplacian would then read :

$$(\Delta \mathbf{f})_j = -\sum_i T_{j,i} A_{j,i} f_i + t_j f_j + V_j f_j \tag{77}$$

Where the positive weights are denoted by $T_{j,i} = T_{i,j}$ and $t_j = \sum_i T_{i,j}$. The vertex potentials are V_i. Choosing the weights and potentials at random one could investigate the rôles of diagonal and off diagonal disorder on the spectrum and eigenfunctions, in the limit $V \to \infty$. The question whether a localization transition occurs is open.
iv. The spectra of quantum graphs with equal (or rationally related) edge lengths, are intimately related to the spectra of the underlying discrete graphs. In particular, the spectral properties of discrete d-regular graphs induce interesting features in their quantum analogues, which call for further research [4].

Acknowledgments

The author wishes to express his deep gratitude to Yehonatan Elon, Amit Godel and Idan Oren whose results, thesis and papers were cut-and-pasted to prepare this survey. The work was supported by the Minerva Center for non-linear Physics, the Einstein (Minerva) Center at the Weizmann Institute and the Wales Institute of Mathematical and Computational Sciences) (WIMCS). Grants from EPSRC (grant EP/G021287), ISF (grant 166/09) and BSF (grant 2006065) are acknowledged.

References

[1] Yehonatan Elon, *Eigenvectors of the discrete Laplacian on regular graphsa statistical approach*, J. Phys. A: Math. Theor. **41** (2008), 435203.

[2] Yhonatan Elon, *Gaussian Waves on the Regular Tree*, arXiv:0907.5065v2 [math-ph] (2009).

[3] PhD thesis submitted to the Feinberg School, The Weizmann Institute of Science (2010).

[4] MSc thesis submitted to the Feinberg School, The Weizmann Institute of Science (2009).

[5] Idan Oren , Amit Godel and Uzy Smilansky, *Trace formulae and spectral statistics for discrete Laplacians on regular graphs (I)*, J. Phys. A: Math. Theor. **42** (2009), 415101.

[6] Idan Oren and Uzy Smilansky, *Trace formulae and spectral statistics for discrete Laplacians on regular graphs (II)*, J. Phys. in press (2010).

[7] Uzy Smilansky *Exterior-Interior Duality for Discrete Graphs* J. Phys. A: Math. Theor. **42** (2009), 035101.

[8] Uzy Smilansky, *Quantum Chaos on Discrete Graphs*, J. Phys. A: Math. Theor. **40** (2007), F621–F630.

[9] D. Jakobson, S. Miller, I. Rivin and Z. Rudnick. *Level spacings for regular graphs*, IMA Volumes in Mathematics and its Applications **109** (1999), 317–329.

[10] A. A. Terras, *Arithmetic Quantum Chaos*, IAS/Park City Mathematical Series **12** (2002), 333–375.

[11] S. Hoory, N. Linial, and A. Wigderson *Expander Graphs and Their Applications*, Bulletin (New Series) of the American Mathematical Society **43**, Number 4, (2006), 439–561 S 0273-0979(06)01126–8.

[12] J. Dodziuk and W.S. Kandel *Combinatorial Laplacians and isoperimetric inequality*, in "From local times to global geometry, control and physics", K. D. Ellworthy Ed., Pitman Research Notes in Mathematics Series, **150** (1986), 68–74.

[13] B. Bollobas, Random Graphs, Academic Press, London (1985).

[14] Fan R. K. Chung, *Spectral Graph Theory*, Regional Conference Series in Mathematics **92**, American mathematical Society (1997).

[15] J. Friedman, *Some geometric aspects of graphs and their eigenfunctions*, Duke Math. J. **69** (1993), 487–525.

[16] N. Alon, *Eigenvalues and Expanders*, Combinatorica, **6** (1986), 83–96.

[17] H. Kesten *Symmetric random walks on groups*, Trans. Am. Math. Soc. **92**, 336–354 (1959).

[18] McKay, B. D., *The expected eigenvalue distribution of a random labelled regular graph*, Linear Algebr. Appl. **40**, 203–216 (1981).

[19] M. Ram Murty, Ramanjuan Graphs, J. Ramanujan Math. Soc. **18** (2003), 1–20.

[20] J.E. Avron, A. Raveh and B. Zur, *Adiabtaic quantum transport in multiply connected systems*, Reviews of Modern Physics **60**, No. 4 (1988).

[21] O. Bohigas, M.-J. Giannoni, and C. Schmit *Characterization of chaotic quantum spectra and universality of level fluctuation laws*, Phys. Rev. Lett. **52** (1984), 1–4.

[22] M.V. Berry and M.Tabor, *Level clustering in the regular spectrum*, Proc. Roy. Soc. A **356** (1977), 375–394.

[23] O. Bohigas, *Random Matrix Theories and Chaotic Dynamics*, in *chaos and quantum physics*, M.J. Giannoni, A. Voros and J. Zinn-Justin Editors pp. 87–199.

[24] Fritz Haake, *Quantum Signatures Of Chaos*, Springer-Verlag Berlin and Heidelberg, (2001).

[25] S. Sodin, *The Tracy-Widom law for some sparse random matrices*, arXiv:0903.4295v2 [math-ph] 7 Apr 2009.

[26] M.C. Gutzwiller, J. Math. Phys. **12** (1984), 343.

[27] M. Gutzwiller *Chaos in Classical and Quantum Mechanics* Springer Verlag, New York, (1991).

[28] M.V. Berry, *Semiclassical Theory of Spectral Rigidity*, Proceedings of the Royal Society of London. Series A, Mathematical and Physical Sciences, Vol. 400, No. 1819 (Aug. 8, 1985), pp. 229-251

[29] N. Argaman, F. Dittes , E. Doron, J. Keating, A. Kitaev, M. Sieber and U. Smilansky. *Correlations in the Acions of Periodic Orbits Derived from Quantum Chaos*. Phys. Rev. Letters **71** (1993), 4326–4329.

[30] M. Sieber, K. Richter, *Correlations between Periodic Orbits and their Rôle in Spectral Statistics*, Physica Scripta, Volume T90, Issue 1, pp. 128-133.

[31] S. Heusler, S. Muller, P. Braun, and F. Haake, *Universal spectral form factor for chaotic dynamics*, J. Phys. A **37** (2004), L31.

[32] H. Bass, *The Ihara -Selberg zeta function of a tree lattice*, Internat. J. Math. **3** (1992), 717–797.

[33] L. Bartholdi, *Counting paths in graphs.* Enseign. Math **45** (1999), 83–131.

[34] N. Alon, I. Benjamini, E. Lubetzky, S. Sodin, *Non-backtracking random walks mix faster*, arXiv:math/0610550v1.

[35] P. Mnëv *Discrete Path Integral Approach to the Selberg Trace Formula for Regular Graphs*, Commun. Math. Phys. **274** (2007), 233–241.

[36] S. Janson, T. ŁUcZak and A. Ruciński,*Random Graphs*, John Wiley & Sons, Inc. (2000).

[37] N.C. Wormald, *The asymptotic distribution of short cycles in random regular graphs*, J. Combin. Theory, Ser. B **31** (1981), 168–182.

[38] B. Bollobás, *A probabilistic proof of an asymptotic formula for the number of labelled regular graphs*, European J. Combin. **1** (1980), 311–316.

[39] B.D. McKay, N.C. Wormald and B. Wysocka, *Short cycles in random regular graphs*, The electronic journal of combinatorics, **11**, R66.

[40] J.P. Keating and N.C. Snaith, *Random Matrix Theory and* $\zeta(1/2+it)$, Commun. Math. Phys. **214**, 57–89 (2000).

[41] A.I. Shnirelman, *Ergodic properties of eigenfunctions*, Uspehi Mat. Nauk **29** (6(180)) (1974), 181–182.

[42] E. J. Heller 1984 Phys. Rev. Lett. **53** 1515.

[43] M.V. Berry, J. Phys. A **10** (1977), 2083–2091.

[44] R. Courant, Nachr. Ges. Wiss. Gttingen, Math. Phys. Kl. (1923).

[45] Galya Blum, Sven Gnutzmann, and Uzy Smilansky, *Nodal Domains Statistics: A Criterion for Quantum Chaos*, Phys. Rev. Lett. **88** (2002),114101.

[46] E. Bogomolny and C. Schmit, Phys. Rev. Lett. **88** (2002), 114102.

[47] Geoffrey Grimmett, Percolation, 2nd Edition, Grundlehren der mathematischen Wissenschaften, vol 321, Springer, (1999).

[48] R. Blümel and U. Smilansky, *Random matrix description of chaotic scattering: Semi Classical Approach.* Phys. Rev. Lett. **64** (1990), 241–244.

[49] E. Doron, U. Smilansky and A. Frenkel. *Chaotic scattering and transmission fluctuations*. Physica D **50** (1991), 367–390.

[50] T. Kottos and U. Smilansky, Quantum Graphs: A simple model for Chaotic Scattering. J. Phys. A. **36** (2003), 3501–3524.

[51] S. Fedorov and B. Pavlov, *Discrete wave scattering on star-graph*. J. Phys. A: Math. Gen. **39** (2006), 2657–2671.

[52] E. B. Curtis and J. A. Morrow, *The Dirichlet to Neumann map for a resistor network* SIAM Journal on Applied Mathematics **51** (1991), 1011–1029.

[53] T. Kottos and U. Smilansky, *Quantum Chaos on Graphs*, Phys. Rev. Lett. **79** (1997), 4794–4797.

[54] T. Kottos and U. Smilansky, *Periodic orbit theory and spectral statistics for quantum graphs*, Annals of Physics **274** (1999), 76–124.

[55] Sven Gnutzmann and Uzy Smilansky, *Quantum Graphs: Applications to Quantum Chaos and Universal Spectral Statistics*, Advances in Physics bf 55 (2006), 527–625.

[56] R. Brooks, Ann. Inst. Fourier **49** (1999), 707–725.